FERMILAB-CONF-10-244-T

MCFM for the Tevatron and the LHC

John M. Campbell[a] and R. K. Ellis[a]

[a]Fermilab, P.O. Box 500, Batavia, IL 60510, USA

A summary is given of the current status of the next-to-leading order (NLO) parton-level integrator MCFM. Some details are given about the Higgs + 2-jet process and the production and decay of $t\bar{t}$, both of which have recently been added to the code. Using MCFM, comparisons between the Tevatron running at $\sqrt{s} = 2$ TeV and the LHC running at $\sqrt{s} = 7$ TeV are made for standard model process including the production of Higgs bosons. The case for running the Tevatron until 16fb^{-1} are accumulated by both detectors is sketched.

1. MCFM

MCFM is a parton-level event integrator which gives results for a series of processes, especially those containing the bosons W, Z and H and heavy quarks, c, b and t. Most processes are included at next-to-leading order (NLO) and include spin correlations in the decay. Table 1 gives an abbreviated summary of the processes which are currently treated by the program. Full documentation for the program is available at ref. [1]. We will not review these processes in detail but rather concentrate on the new features which are present in version 5.8 which was released in April 2010.

Table 1
Abbreviated summary of MCFM proceses

Final state	Notes	Ref.
W/Z processes		
W/Z		
$WW/ZZ/WZ$		[2]
$Wb\bar{b}$	$m_b = 0$	[3]
$Zb\bar{b}$	$m_b = 0$	[4]
$W/Z + 1$ jet		
$W/Z + 2$ jets		[5]
Wc	$m_c \neq 0$	[6]
Zb	$n_f = 5$	[7]
Zb+jet	$n_f = 5$	[8]
H processes		
H(g.f.)		
H+1 jet(g.f.)		
H+2 jets (g.f.)	$m_t \to \infty$	[9,10,11]
WH/ZH		
H via WBF		[12]
Hb	$n_f = 5$	[13]
t processes		
t	s and t channel	[14]
t	t channel,$n_f = 4$	[15,16]
Wt	$n_f = 5$	[6]
$t\bar{t}$	with t decay	
Processes not present in released version		
Wb +jet		[17,18]
WW +jet		[19]
J/ψ & Υ		[20]
$\gamma N \to J/\psi$		[21]

2. Higgs + two jets

A new process which is in MCFM version 5.8 is the production of a Higgs boson in association with two jets. Sample diagrams contributing to Higgs boson production are shown in Fig. 1. We shall focus on the process in Fig. 1(c) and other Higgs + 4 parton processes, which can be considered a background to the vector boson fusion process, Fig. 1(d). The calculations underlying our implementation are performed at NLO using an effective Lagrangian to express the coupling of gluons to the Higgs field [22],

$$\mathcal{L}_H^{\rm int} = \frac{C}{2} H \,{\rm tr}\, G_{\mu\nu} G^{\mu\nu} , \qquad (1)$$

where the trace is over the color degrees of freedom. At NLO the coefficient C is given in the $\overline{\rm MS}$ scheme by [23,24],

$$C = \frac{\alpha_S}{6\pi v}\Big(1 + \frac{11}{4\pi}\alpha_S\Big) + \mathcal{O}(\alpha_S^3) . \qquad (2)$$

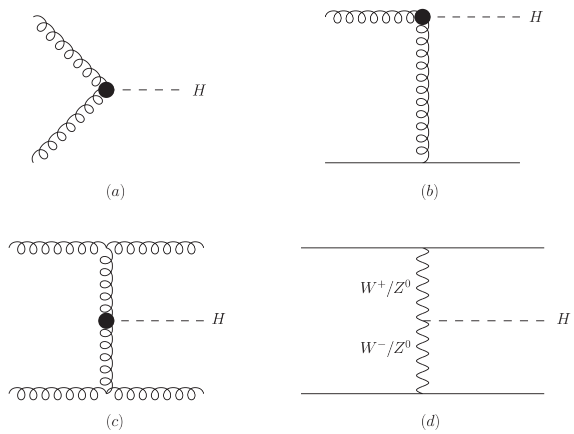

Figure 1. Higgs production processes at lowest order.

Here v is the vacuum expectation value of the Higgs field, $v = 246$ GeV. Phenomenological results on this process at NLO were first published in ref. [9] using a semi-numerical method to calculate the virtual corrections. Here we shall present new phenomenological results for the Higgs + 2 jet process, based on analytic calculations of the one-loop Higgs + 4 parton amplitudes which have recently been completed. The use of analytic results leads to a considerable improvement in the speed of the code.

2.0.1. One-loop H + 4 parton amplitudes

The effective Lagrangian used in the calculation of the Higgs + 4 parton amplitudes was simplified by introducing a complex scalar field [25],

$$\phi = \frac{1}{2}\left(H + iA\right), \quad \phi^\dagger = \frac{1}{2}\left(H - iA\right) \ , \qquad (3)$$

so that the effective Lagrangian, Eq. (1), can be written as,

$$\mathcal{L}^{\rm int}_{H,A} = \frac{C}{2}\Big[H \ {\rm tr}\, G_{\mu\nu}\, G^{\mu\nu} + iA \ {\rm tr}\, G_{\mu\nu}\, {}^*G^{\mu\nu}\Big] = \\ = \ C\Big[\phi \ {\rm tr}\, G_{SD\ \mu\nu}\, G^{\mu\nu}_{SD} + \phi^\dagger \ {\rm tr}\, G_{ASD\ \mu\nu}\, G^{\mu\nu}_{ASD}\Big].$$

Table 2
Comparison of calculations of refs. [31,10]

ADGSW[31]	LO	NLO	NNLO
Higgs+0jet	✓	✓	✓
Higgs+1jet	✓	✓	
Higgs+2jet	✓		
CEW [10]	**LO**	**NLO**	**NNLO**
Higgs+0jet	✓	✓	
Higgs+1jet	✓	✓	
Higgs+2jet	✓	✓	

The gluon field strength has been separated into a self-dual and an anti-self-dual component,

$$G^{\mu\nu}_{SD} = \frac{1}{2}(G^{\mu\nu} + {}^*G^{\mu\nu}), G^{\mu\nu}_{ASD} = \frac{1}{2}(G^{\mu\nu} - {}^*G^{\mu\nu}) \\ {}^*G^{\mu\nu} \equiv \frac{i}{2}\varepsilon^{\mu\nu\rho\sigma} G_{\rho\sigma} \ . \qquad (4)$$

Calculations performed in terms of the field ϕ are simpler than the calculations for the Higgs boson and, moreover, the amplitudes for $\phi^\dagger$ can be obtained from the ϕ amplitudes by using parity. The full Higgs boson amplitude is written as a combination of ϕ and $\phi^\dagger$ components:

$$A(H) = A(\phi) + A(\phi^\dagger) \ . \qquad (5)$$

A nice summary of all the one-loop results for the Higgs + 4 gluon amplitudes is given in ref. [26]. Full references for the analytic calculations of the $H\bar{q}qgg$ amplitudes can be found in ref. [28]. Results for the matrix squared for the $Hq\bar{q}q\bar{q}$ process are given in ref. [9] and for the amplitude in ref. [27].

2.1. Phenomenological impact

In addition to its importance at the LHC, the Higgs + 2 jet cross section is also important at the Tevatron. The experiments [30] analyze the events with different numbers of jets separately to make maximal use of the different kinematic structure. In the spirit of Ref. [31], we can refine the estimate of the theoretical uncertainty on the number of Higgs signal events originating from QCD parton fusion processes

In Table 2 we contrast the two different approaches to calculating the Higgs + 2 jet cross sections of Ref. [31] and Ref. [10]. Ref. [31] is in

Table 3
LO and NLO Higgs + two jet cross section at $\sqrt{s} = 1.96$ TeV, together with theoretical errors.

m_H[GeV]	Γ_H[GeV]	σ_{LO}[fb]	σ_{NLO}[fb]
160	0.0826	$0.345^{+92\%}_{-44\%}$	$0.476^{+35\%}_{-31\%}$

essence a NNLO calculation of the total cross section, which as a byproduct includes the Higgs + 2 jet process in leading order. The MCFM implementation [10] only calculates the Higgs + 0 jet cross section at NLO, but also includes the Higgs + 2 jet cross section at NLO.

By using the fractions of the Higgs cross section in the different multiplicity bins taken from Ref. [32], we can update Eq. (4.3) of Ref. [31] (for a Higgs boson of mass 160 GeV) with,

$$\frac{\Delta N(\text{scale})}{N} = \begin{pmatrix} +13.8\% \\ -15.5\% \end{pmatrix} = 60\% \cdot \begin{pmatrix} +5\% \\ -9\% \end{pmatrix} + 29\% \cdot \begin{pmatrix} +24\% \\ -23\% \end{pmatrix} + 11\% \cdot \begin{pmatrix} +35\% \\ -31\% \end{pmatrix} \quad (6)$$

Only the uncertainty on the Higgs + ≥ 2 jet bin, (which is only 11% of the total) has been modified, using the results from Table 3.

The corresponding determination using the uncertainty derived from the LO result for the Higgs + $\geq$ 2 jet bin is $(+20,0\%, -16.9\%)$ [31], so the result in Eq. (6) represents a modest improvement in the overall theoretical error, but one which will have implications for the Higgs search at the Tevatron.

3. Top production and decay

Another new process which is included at NLO is the production of pairs of top quarks including the decay. The top quarks are kept strictly on their mass shell, so the processes of production and decay are separately gauge invariant, but full spin correlations are kept. Although this is not a new result [35,36], it is importantant to include it in the MCFM package because top pair production is such an important background for many processes at hadron colliders. We can assess the importance of including these spin correlations by looking at the angular separation of the two charged leptons coming from top decay. The expected data sample of top quark pairs at $\sqrt{s} = 7$ TeV will be too small to observe these correlations, but they should be observable at $\sqrt{s} = 14$ TeV. Fig. 2 shows the azimuthal angle ϕ in the transverse plane between the two charged leptons in top pair production events. In addition to standard lepton and jet cuts, $p_{T,l} > 20$ GeV, $p_{T,bjet} > 25$ GeV, $p_{T,miss} > 40$ GeV, $\eta_l, \eta_{bjet} < 2.5$ we apply the cut $p_{T,l} < 50$ GeV to constrain the top quarks to be produced close to threshold [37]. These specific cuts have been suggested by Schulze [38].

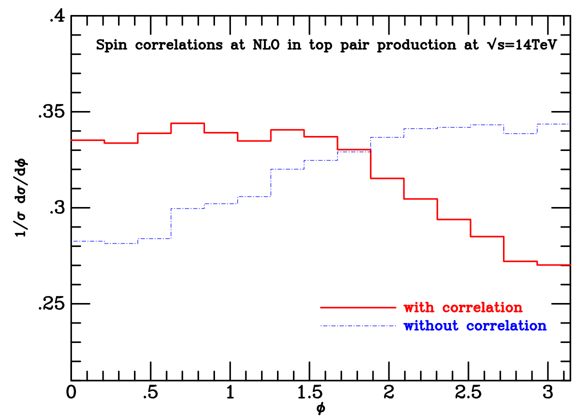

Figure 2. Effect of spin correlations in top decay.

4. Run III at the Tevatron

The basic ratios of cross sections are governed by the parton luminosities. Fig. 3 shows the ratios of parton luminosities in pp collisions at $\sqrt{s} = 14, 10$ and 7 TeV compared to the luminosity in $p\bar{p}$ collisions at $\sqrt{s} = 2$ TeV. Considering in detail the case of 7 TeV, in the range $\sqrt{\hat{s}} = 100 - 200$ GeV the $u\bar{d}$ luminosity goes up by a factor of $4 - 5$ whereas the gg luminosity grows by at least a factor of 15. This means that for $q\bar{q}$ induced processes the Tevatron has a competitive advantage. That is, in a scenario where the Tevatron has an accumulated luminosity of 10 fb^{-1} and the LHC has an accumulated luminosity of 1 fb^{-1} at $\sqrt{s} = 7$ TeV, the Tevatron still has a competitive advantage for $q\bar{q}$ induced processes.

We now further discuss the situation if the Tevatron were to run for three further years after 2011; after this period the experiments would have accumulated 16 fb^{-1} per experiment of analyzeable luminosity. Fig. 4 shows the number of events produced for various standard model processes, assuming 16 fb^{-1} of accumulated luminosity for the Tevatron and 1 fb^{-1} of accumulated luminosity for the LHC. In this situation the Tevatron would have a clear advantage for $q\bar{q}$ initiated processes.

The situation with regard to the standard model Higgs boson is interesting, since at the Tevatron the low mass Higgs boson is sought in association with a vector boson V in the $q\bar{q}$-initiated mode $q\bar{q} \to VH$. If we take the precision standard model fits [33] seriously, the standard model 2σ-allowed region for the Higgs boson mass is $114 < M_H < 145$ GeV. In this region the primary decay of the Higgs boson is into $b\bar{b}$, a channel which is not expected to be observable at the LHC until 30 fb^{-1} have been accumulated at $\sqrt{s} = 14$ TeV [34].

If the Tevatron were to accumulate 16 fb^{-1} of analyzeable luminosity, per experiment it could provide 3σ evidence for the standard model Higgs boson in the range $100 < m_H < 180$ GeV [39]. This is an important goal, which would provide complementary information to the information on the decay $H \to \gamma\gamma$ which will be available from 14 TeV running at the LHC.

5. Conclusions

This year has been mainly a consolidation period for MCFM, but with the introduction of two new processes at NLO, top pair production with decay and the Higgs boson + 2 jet production at the LHC.

Using MCFM it has been shown that the Tevatron can provide important information on $q\bar{q}$ initiated processes, and that for these processes it will be superior to the LHC until considerable data has been accumulated at $\sqrt{s} = 14$ TeV. An important example is the Higgs boson where the $H \to b\bar{b}$ decay of the low mass Higgs can be looked for. Information in this channel is complementary to the information from the LHC and probably unique until at least 2015.

REFERENCES

1. J. M. Campbell and R. K. Ellis, MCFM home page, http://mcfm.fnal.gov
2. J. M. Campbell and R. K. Ellis, Phys. Rev. D **60**, 113006 (1999) [arXiv:hep-ph/9905386].
3. R. K. Ellis and S. Veseli, Phys. Rev. D **60**, 011501 (1999) [arXiv:hep-ph/9810489].
4. J. M. Campbell and R. K. Ellis, Phys. Rev. D **62**, 114012 (2000) [arXiv:hep-ph/0006304].
5. J. M. Campbell and R. K. Ellis, Phys. Rev. D **65**, 113007 (2002) [arXiv:hep-ph/0202176].
6. J. M. Campbell and F. Tramontano, Nucl. Phys. B **726**, 109 (2005) [arXiv:hep-ph/0506289].
7. J. M. Campbell, R. K. Ellis, F. Maltoni and S. Willenbrock, Phys. Rev. D **69**, 074021 (2004) [arXiv:hep-ph/0312024].
8. J. M. Campbell, R. K. Ellis, F. Maltoni and S. Willenbrock, Phys. Rev. D **73**, 054007 (2006) [Erratum-ibid. D **77**, 019903 (2008)] [arXiv:hep-ph/0510362].
9. J. M. Campbell, R. K. Ellis and G. Zanderighi, JHEP **0610**, 028 (2006) [arXiv:hep-ph/0608194].
10. J. M. Campbell, R. K. Ellis and C. Williams, Phys. Rev. D **81**, 074023 (2010) [arXiv:1001.4495 [hep-ph]].
11. J. M. Campbell, R. K. Ellis and C. Williams, arXiv:1005.3733 [hep-ph].
12. E. L. Berger and J. M. Campbell, Phys. Rev. D **70**, 073011 (2004) [arXiv:hep-ph/0403194].
13. J. M. Campbell, R. K. Ellis, F. Maltoni and S. Willenbrock, Phys. Rev. D **67**, 095002 (2003) [arXiv:hep-ph/0204093].
14. J. M. Campbell, R. K. Ellis and F. Tramontano, Phys. Rev. D **70**, 094012 (2004) [arXiv:hep-ph/0408158].
15. J. M. Campbell, R. Frederix, F. Maltoni and F. Tramontano, Phys. Rev. Lett. **102**, 182003 (2009) [arXiv:0903.0005 [hep-ph]].
16. J. M. Campbell, R. Frederix, F. Maltoni and F. Tramontano, JHEP **0910**, 042 (2009)

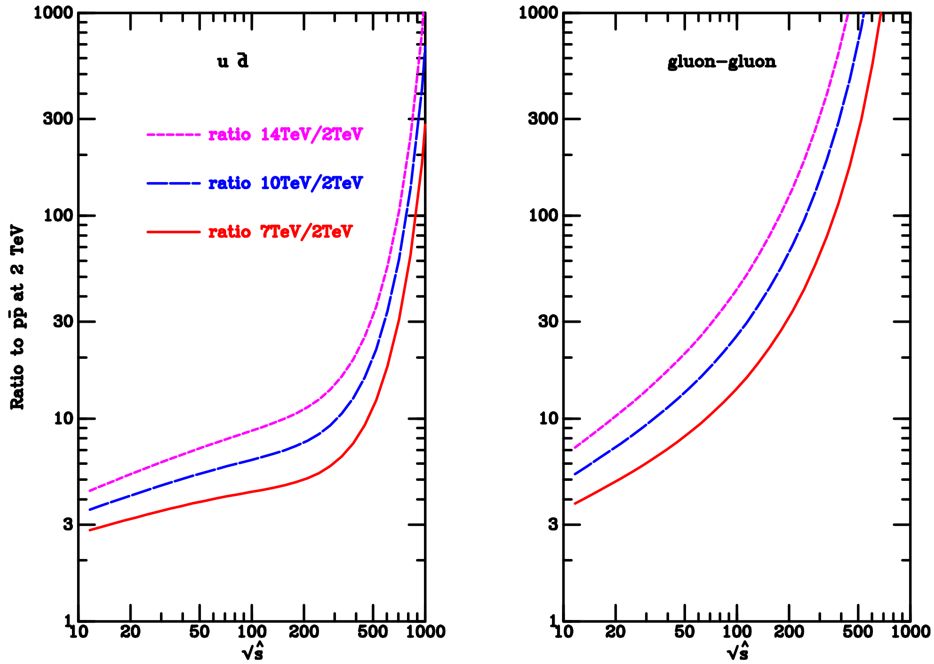

Figure 3. Ratios of luminosities at $\sqrt{s}$=7, 10 and 14 TeV, compared with $p\bar{p}$ at $\sqrt{s}$=2 TeV

[arXiv:0907.3933 [hep-ph]].
17. J. M. Campbell, R. K. Ellis, F. Maltoni and S. Willenbrock, Phys. Rev. D **75**, 054015 (2007) [arXiv:hep-ph/0611348].
18. J. M. Campbell, R. K. Ellis, F. Febres Cordero, F. Maltoni, L. Reina, D. Wackeroth and S. Willenbrock, Phys. Rev. D **79**, 034023 (2009) [arXiv:0809.3003 [hep-ph]].
19. J. M. Campbell, R. K. Ellis and G. Zanderighi, JHEP **0712**, 056 (2007) [arXiv:0710.1832 [hep-ph]].
20. J. M. Campbell, F. Maltoni and F. Tramontano, Phys. Rev. Lett. **98**, 252002 (2007) [arXiv:hep-ph/0703113].
21. P. Artoisenet, J. M. Campbell, F. Maltoni and F. Tramontano, Phys. Rev. Lett. **102**, 142001 (2009) [arXiv:0901.4352 [hep-ph]].
22. F. Wilczek, Phys. Rev. Lett. **39**, 1304 (1977).
23. A. Djouadi, M. Spira and P. M. Zerwas, Phys. Lett. B **264**, 440 (1991).
24. S. Dawson, Nucl. Phys. B **359**, 283 (1991).
25. L. J. Dixon, E. W. N. Glover and V. V. Khoze, JHEP **0412**, 015 (2004) [arXiv:hep-th/0411092].
26. S. Badger, E. W. N. Glover, P. Mastrolia and C. Williams, arXiv:0909.4475 [hep-ph].
27. L. J. Dixon and Y. Sofianatos, arXiv:0906.0008 [hep-ph].
28. S. Badger, J. M. Campbell, R. K. Ellis and C. Williams, JHEP **0912**, 035 (2009) [arXiv:0910.4481 [hep-ph]].
29. V. Del Duca, A. Frizzo and F. Maltoni, JHEP **0405**, 064 (2004) [arXiv:hep-ph/0404013].
30. T. Aaltonen *et al.* [CDF Collaboration and D0 Collaboration], arXiv:1005.3216 [hep-ex].
31. C. Anastasiou, G. Dissertori, M. Grazzini, F. Stockli and B. R. Webber, JHEP **0908**, 099 (2009) [arXiv:0905.3529 [hep-ph]].
32. CDF collaboration, "Search for $H \to WW^{\star}$ production at CDF using 3.0 fb^{-1} of data," CDF note 9500.
33. H. Flacher, M. Goebel, J. Haller, A. Hocker,

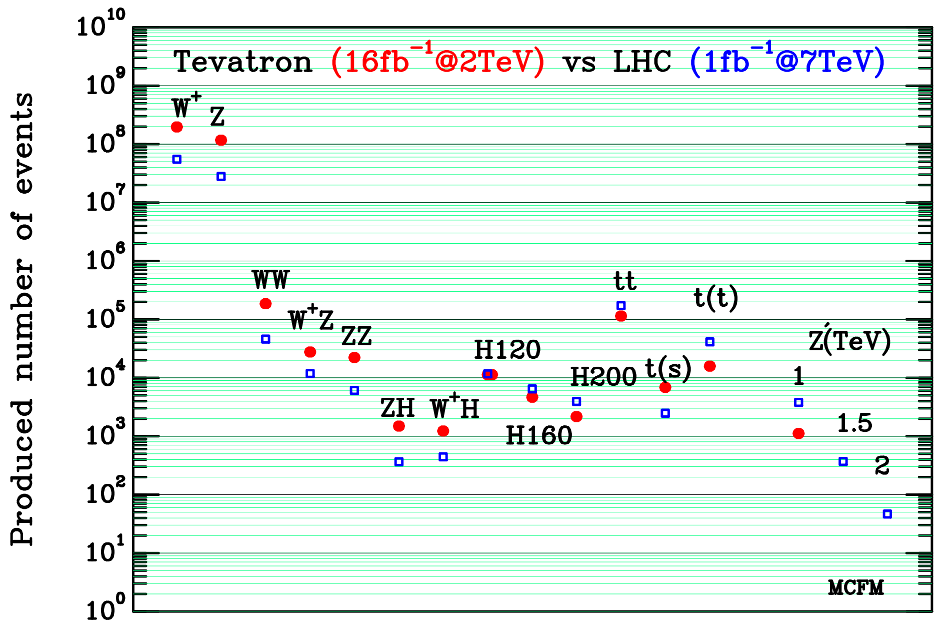

Figure 4. Number of events for production of W, Z Higgs, top pair, single top, and Z' at $\sqrt{s} = 2$ and 7 TeV. Efficiencies are assumed to be 100%.

K. Moenig and J. Stelzer, Eur. Phys. J. C **60**, 543 (2009) [arXiv:0811.0009 [hep-ph]].

34. J. M. Butterworth, A. R. Davison, M. Rubin and G. P. Salam, Phys. Rev. Lett. **100**, 242001 (2008) [arXiv:0802.2470 [hep-ph]].
35. W. Bernreuther, A. Brandenburg, Z. G. Si and P. Uwer, Phys. Rev. Lett. **87**, 242002 (2001) [arXiv:hep-ph/0107086].
36. K. Melnikov and M. Schulze, JHEP **0908**, 049 (2009) [arXiv:0907.3090 [hep-ph]].
37. G. Mahlon and S. J. Parke, Phys. Rev. D **81**, 074024 (2010) [arXiv:1001.3422 [hep-ph]].
38. M. Schulze, talk presented at Loopfest 2010.
39. see, for example, J. Konigsberg, Proceedings of Les Rencontres de Physique de la Vallée d'Aoste (La Thuile 2010).